Diamond Like Carbon for the Fast Timing MPGD

Piet Verwilligen
INFN sez. Bari

DLC from a user's perspective

Seminario
October 29th 2018, CEDAD

Micro Pattern Gaseous Detectors

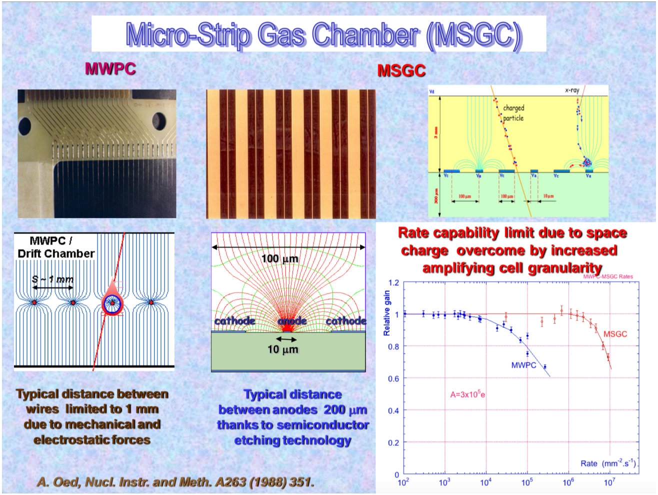

MPGD Detection Principle

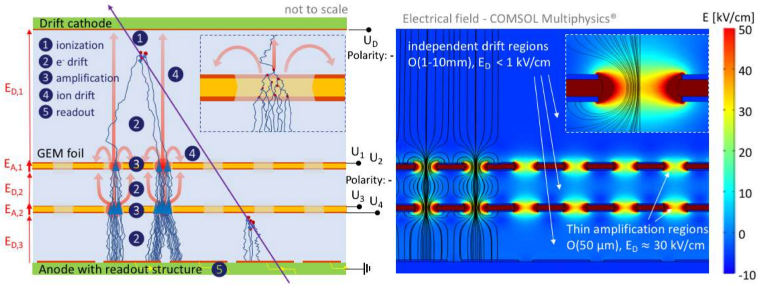

Figure 1.5.: Left: Layout of a double stage GEM detector and signal formation processes triggered by a trespassing muon (purple). The electrons (blue) freed along the track are guided into the GEM holes, where they are amplified, extracted on the other side and further amplified in the second GEM. The ion flow (red arrows) is indicated. The primary cluster number and charge densities are not to scale. Right: Electric field configuration in the GEM stack with the extended drift regions, confined amplification volumes and exemplary streamlines to indicate charge drift.

Who uses MPGDs?

CERN Courier (5 pages) Volume, October 2015

CERN Courier October 2015

Detector R&D

RD51 and the rise of micro-pattern gas detectors

Since its foundation, the RD51 collaboration has provided important stimulus for the development of MPGDs.

Improvements in detector technology often come from capitalizing on industrial progress. Over the past two decades, advances in photolithography, microelectronics and printed circuits have opened the way for the production of micro-structured gas-amplification devices. By 2008, interest in the development and use of the novel micro-pattern gaseous detector (MPGD) technologies led to the establishment at CERN of the RD51 collaboration. Originally created for a five-year term, RD51 was later prolonged for another five years beyond 2013. While many of the MPGD technologies were introduced before RD51 was founded (figure 1), with more techniques becoming available or affordable, new detection concepts are still being introduced, and existing ones are substantially improved.

In the late 1980s, the development of the micro-strip gas chamber (MSGC) created great interest because of its intrinsic rate-capability, which was orders of magnitude higher than in wire chambers, and its position resolution of a few tens of micrometres at particle fluxes exceeding about 1 MHz/mm^2. Developed for projects at high-luminosity colliders, MSGCs promised to fill a gap between the high-performance but expensive solid-state detectors, and cheap but rate-limited traditional wire chambers. However, detailed studies of their long-term behaviour at high rates and in hadron beams revealed two possible weaknesses of the MSGC technology: the formation of deposits on the electrodes, affecting gain and performance ("ageing effects"), and spark-induced damage to electrodes in the presence of highly ionizing particles.

These initial ideas have since led to more robust MPGD structures, in general using modern photolithographic processes on thin insulating supports. In particular, ease of manufacturing, operational stability and superior performances for charged-particle tracking, muon detection and triggering have given rise to two main designs: the gas electron-multiplier (GEM) and the micro-mesh gaseous structure (Micromegas). By using a pitch size of a few hundred micrometres, both devices exhibit intrinsic high-rate capability (> 1 MHz/mm^2), excellent spatial and multi-track resolution (around 30 μm and 500 μm, respectively), and time resolution for single photoelectrons in the sub-nanosecond range.

Coupling the microelectronics industry and advanced PCB technology has been important for the development of gas detectors with increasingly smaller pitch size. An elegant example is the use of a CMOS pixel ASIC, assembled directly below the GEM or Micromegas amplification structure. Modern "wafer post-processing technology" allows for the integration of a Micromegas grid directly on top of a Medipix or Timepix chip, thus forming

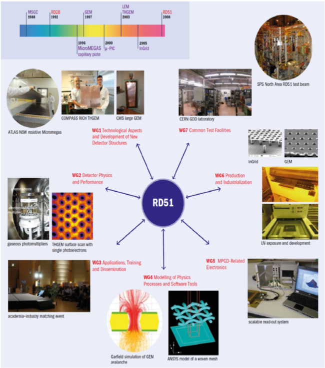

Fig.1. The seven working groups of RD51, with illustrations of just a few examples of the different kinds of work involved. Top left: the 20-year pre-history of RD51. (Image credits: RD51 Collaboration.)

integrated read-out of a gaseous detector (InGrid). Using this approach, MPGD-based detectors can reach the level of integration, compactness and resolving power typical of solid-state pixel devices. For applications requiring imaging detectors with large-area coverage and moderate spatial resolution (e.g. ring-imaging Cherenkov (RICH) counters), coarser macro-patterned structures offer an interesting economic solution with relatively low mass and easy construction – thanks to the intrinsic robustness of the PCB electrodes. Such detectors are the thick GEM (THGEM), large electron multiplier (LEM), patterned resistive thick GEM (RETGEM) and the resistive-plate WELL (RPWELL).

RD51 and its working groups

The main objective of RD51 is to advance the technological development and application of MPGDs. While a number of activities have emerged related to the LHC upgrade, most importantly, RD51 serves as an access point to MPGD "know-how" for the world-wide community – a platform for sharing information, results and experience – and optimizes the cost of R&D through the sharing of resources and the creation of common projects and infrastructure. All partners are already pursuing either basic- or application-oriented R&D involving MPGD concepts. Figure 1 shows the organization of seven Working Groups (WG) that cover all of the relevant aspects of MPGD-related R&D.

WG1 Technological Aspects and Development of New Detector Structures. The objectives of WG1 are to improve the performance of existing detector structures, optimize fabrication methods, and develop new multiplier geometries and techniques. One of the most prominent activities is the development of large-area GEM, Micromegas and THGEM detectors. Only one decade ago, the largest MPGDs were around 40 × 40 cm^2, limited by existing tools and materials. A big step towards the industrial manufacturing of MPGDs with a size around a square metre came with new fabrication methods – the single-mask GEM, "bulk" Micromegas, and the novel Micromegas construction scheme with a "floating mesh". While in "bulk" Micromegas, the metallic mesh is integrated into the PCB read-out, in the "floating-mesh" scheme it is integrated in the panel containing drift electrodes and placed on pillars when the chamber is closed. The single-mask GEM technique overcomes the cumbersome practice of alignment of two masks between top and bottom films, which limits the achievable lateral size to 50 cm. This technology, together with the novel "self-stretching technique" for assembling GEMs without glue and spacers, simplifies the fabrication process to such an extent that, especially for large-volume production, the cost per unit area drops by orders of magnitude. ▷

Maxim Titov & Leszek Ropelewski

Who uses MPGDs?

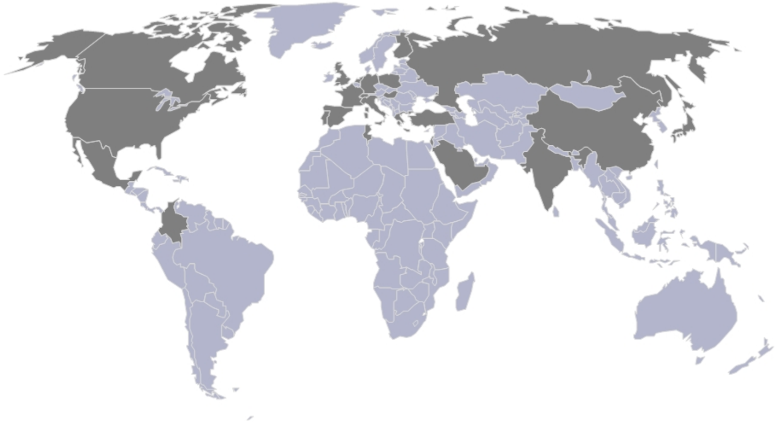

$\sim$ **450 authors, 75 institutes, 25 countries**

Who uses MPGDs?

MPGDs at the forefront of Gas Detector R&D

MPGDs: e.g. Gas Electron Multiplier (GEM)

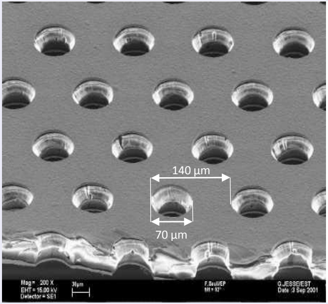

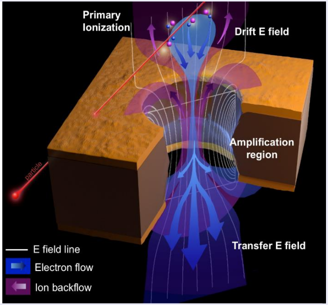

Characteristics: OK for HL-LHC, μ-tomography

- High rate capability ($> 50\,\text{MHz/cm}^2$), Good spatial resolution ($50\,\mu$m), High efficiency ($\geq 95\,\%$), Flexible detector structures, Time resolution of $\mathcal{O}(5\text{–}10\,\text{ns})$

Missing: Needed for FCC, TOF-PET, . . .

- **Spark protection** ($\rightarrow$ Resistive Materials) & **Time resolution** in range 25 ps – 1 ns

Fast Timing MPGD Principle

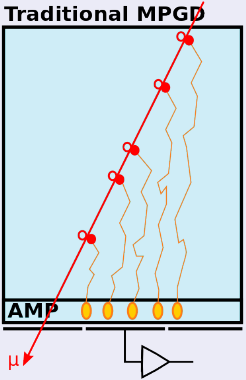

σ_t driven by distance fluct's

$$\boxed{\begin{array}{c}\sigma_t \propto 1/(\lambda v_{\text{drift}}) \\ \lambda = \#\text{ primary cls / mm}\end{array}}$$

electron-ion pairs created close to amplification structure result in fast signals

Fast Timing MPGD: split drift volume in N layers, each with own amplification structure

$$\boxed{\sigma_t \propto 1/(\lambda v_{\text{drift}} N)}$$

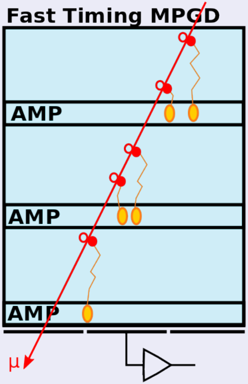

- *slow drift velocity:* $v_d = 70\,\mu m/ns$ $\quad$ *[Ar:CO_2 (70:30) @3 kV/cm]*
- *number of primary ionizations:* $\lambda = 2.5\ mm^{-1} \Rightarrow \sigma_t = 5.7\ ns$
- $P(x \geq a) = \int_a^\infty \exp(-\lambda x')\,dx' = 0.5 \Rightarrow a \geq 277\,\mu m \,\widehat{=}\, 3.95\,ns$

Fast Timing MPGD Principle

Traditional MPGD

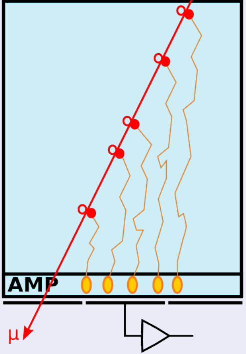

σ_t driven by distance fluct's

$$\boxed{\begin{array}{c}\sigma_t \propto 1/(\lambda v_{\text{drift}}) \\ \lambda = \#\ \text{primary cls / mm}\end{array}}$$

electron-ion pairs created close to amplification structure result in fast signals

Fast Timing MPGD: split drift volume in N layers, each with own amplification structure

$$\boxed{\sigma_t \propto 1/(\lambda v_{\text{drift}} N)}$$

Fast Timing MPGD

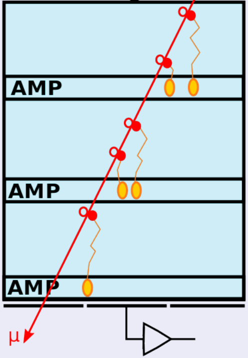

- **resistive structure $\Rightarrow$ signal from any layer induced in readout**
- **resistive structure $\Rightarrow$ limits development of discharges**
- **time resolution improves with N = number of layers**

Two Layer FTM Prototype :: Design

2-layer prototype

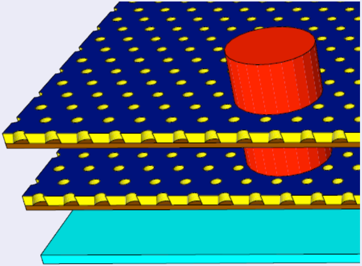

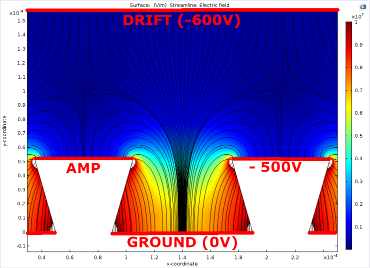

Single layer specifications:

- Drift layer: 250 μm drift layer (Red: Dupont Coverlay spacers)
- Gain layer: 50 μm kapton (Yellow: GEM foil: 70 μm hole, 140 μm pitch)
- Resistive kapton: 25 μm (Brown: Dupont high resistivity Kapton XC)
- Resistive coating: 10–100 nm (Blue: Diamond Like Carbon: DLC)

Two Layer FTM Prototype :: Design

2-layer prototype

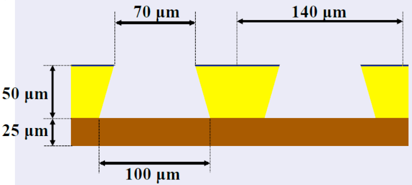

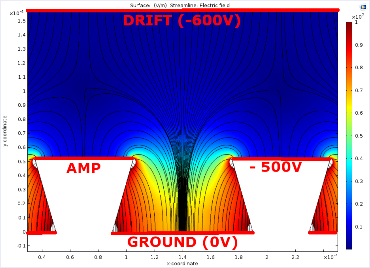

Single layer specifications:

- Drift layer: 250 μm drift layer (Red: Dupont Coverlay spacers)
- Gain layer: 50 μm kapton (Yellow: GEM foil: 70 μm hole, 140 μm pitch)
- Resistive kapton: 25 μm (Brown: Dupont high resistivity Kapton XC)
- Resistive coating: 10–100 nm (Blue: Diamond Like Carbon: DLC)

(intrinsic) FTM Challenges

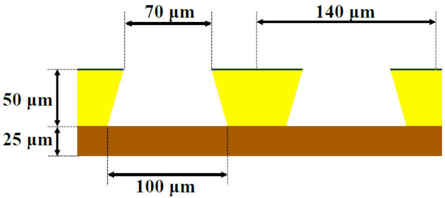

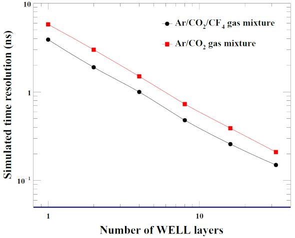

FTM requirements:

- detection of single ionization-e^- instead of all e^- in drift *(charge ÷ 10-30)*
- detection with single amplification structure that has very high gain $(10^4 - 10^5)$

Therefore:

⇒ need high gain structure, with low spark/discharge rate (⇒ resistive electrodes)

⇒ need fast electronics that can process pulse with low charge $(10^4 e^- = 1.6\ fC)$
does not exist — typically high gain detectors are used for fast timing — $\sigma_t \propto t_{rise} \div S/N$

Signal Transparency vs Resistivity

RESISTIVE CATHODE TRANSPARENCY

G. BATTISTONI, P. CAMPANA, V. CHIARELLA, U. DENNI, E. IAROCCI and G. NICOLETTI
INFN – Laboratori Nazionali di Frascati, Frascati, Italy

Nuclear Instruments and Methods 202 (1982) 459–464
North-Holland Publishing Company

Received 23 February 1982

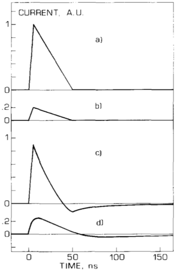

Fig. 6. Pulse shapes on the strip as simulated with the SPICE program, for full transparency (a, b), and for a transparency equal to 0.75 (c, d).

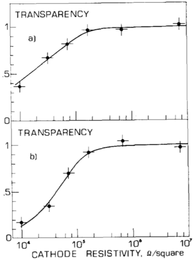

Fig. 4. Cathode transparency as a function of surface resistivity, for 1 cm strips (a) and 2 cm (b). The continuous curves are the results of a calculation.

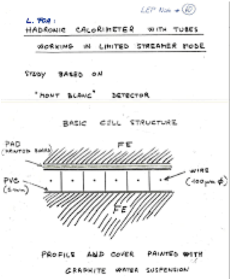

⇒ **Resistive materials with** $R > 200\,\mathrm{k}\Omega/\square$ **are nearly 100% transparent**

Rate Capability vs Resistivity

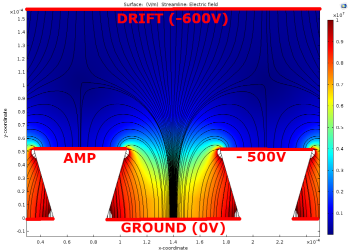

- **Effective Voltage** due to current I and material with resistance $R_e = \rho l/A$:

$$V_{\text{eff}} = V_{\text{app}} - IR_e$$

- with particle **rate** R: $I = \langle q \rangle R$
- **Voltage drop** $\Delta V = \langle q \rangle R \rho l / A$
- E-field $\downarrow$ $\Rightarrow$ detector $\epsilon \downarrow$

P. Fonte et al. / Nuclear Instruments and Methods in Physics Research A 431 (1999) 154–159

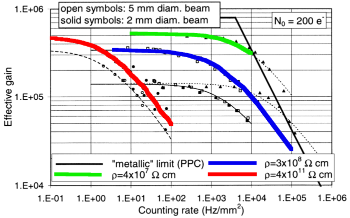

- R_{max} depends on Gain $\propto \langle q \rangle$ and ρ
- **Raether limit** ($q_{\text{max}} = 10^8 e$) $\Rightarrow G \times R = \text{cte}$
- **Typical MPGDs** at $G = \text{few} \times 10^3$ $\Rightarrow$ MSGC $R_{\text{max}} \simeq 100\,\text{MHz cm}^{-2}$
- **CMS RPC** $\rho = (1 \div 6) \times 10^{10}\ \Omega$ cm $\Rightarrow$ (CMS) RPC $R_{\text{max}} \simeq 300\,\text{Hz cm}^{-2}$
- **low-resistive mat.** ($\rho = 4 \times 10^7\ \Omega$ cm $\Rightarrow R_{\text{max}} \simeq 1\,\text{MHz cm}^{-2}$ **@**$G = 10^5$

Charge Spread due to Resistivity

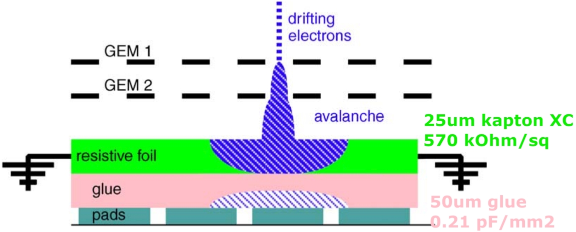

Fig. 1. Schematic of a double GEM test cell designed for charge dispersion studies.

- charge density $\rho(x, y, t)$ defined from:

$$\frac{\partial \rho}{\partial t} = \frac{1}{RC}\left(\frac{\partial^2 \rho}{\partial x^2} + \frac{\partial^2 \rho}{\partial y^2}\right)$$

- pad $2 \times 6\,\mathrm{mm}^2$; $R = R_S \times l/w = 570\,\mathrm{k}\Omega/\square \times 3$; $C = 0.21\,\mathrm{F/mm}^2 \times 12\,\mathrm{mm}^2$

M.S. Dixit — NIM A 566 (2006) 281-285

Charge Spread due to Resistivity

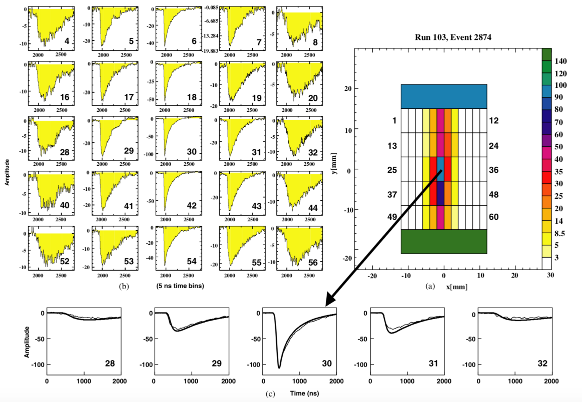

- Vertical Cosmic Ray Muon passing through detector
- Avalanche charge spread $\sim 150\,\mu$m; Observed hit pattern: 10 mm $\times$ 30 mm;
- Charge weighting $\sigma_x \simeq 100\,\mu$m (5% of stripwidth) $[R_S = 570\,\mathrm{k}\Omega/\square]$

M.S. Dixit — NIM A 566 (2006) 281-285

Charge Spread due to Resistivity

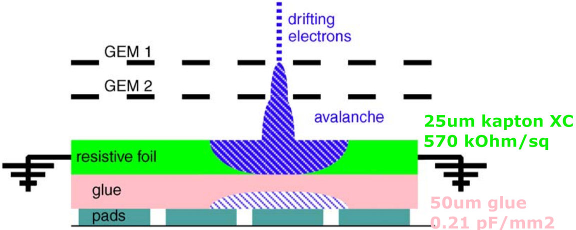

Fig. 1. Schematic of a double GEM test cell designed for charge dispersion studies.

- **Advantage:** Improved position resolution through charge weighting with reduced number of readout-strips
- **Disadvantage:** If spread out over too many readout channels, signal might be below threshold
- **Furthermore:** larger part of the detector might become inactive due to voltage-drop after passing of particle

M.S. Dixit — NIM A 566 (2006) 281-285

Typical Dimensions and Typical Resistivities

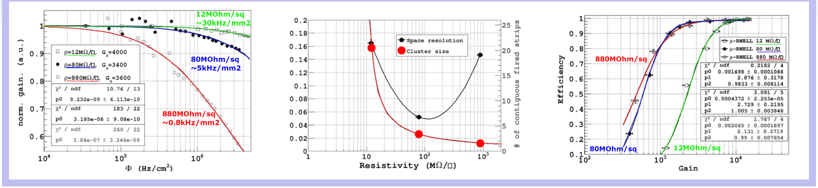

G.Bencivenni NIM A 886 (2018) 36-39

For FTM we would like to have the lowest R that allows for good signal transparency, obtaining as such the highest rate capability, w/o too much charge spread

- Choice of resistivity for an application is a trade-off between various effects:
  - **rate capability:** high resistivity $\Rightarrow$ Large Voltage drop $\Rightarrow$ Low Rate Capability
  - **charge spread:** low resistivity $\Rightarrow$ Large charge spread (need good optimum)
  - **signal transparency:** higher resistivity gives better signal transparency
- **Want to explore MPGDs w/ $R_S = 100\,\mathrm{k}\Omega/\square$—$1\,\mathrm{G}\Omega/\square$, first try $100\,\mathrm{M}\Omega/\square$**

Which Materials can we use?

- Resistive electrodes is one of best choice for reducing the sparks on MPGDs.
- However, it is not easy to find the “resistive material” for Micro Pattern.
- In case, surface resistivity of 1MΩ/sq. is needed;
  - In general, the electrodes for MPGDs has 0.1μm – 10μm thickness.
  - Those correspond to bulk resistivity of 0.1Ωm–10Ωm.

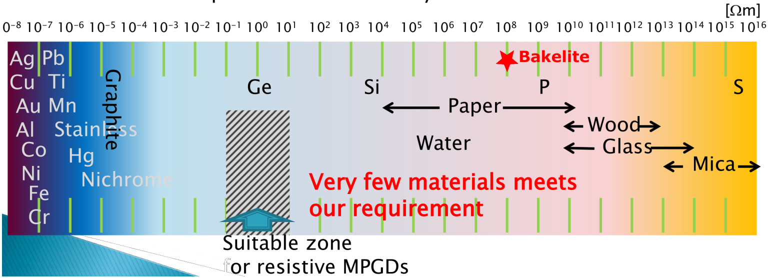

Which Materials can we use?

Conductivity of materials

- Intrinsic materials are divided into insulator and conductors.
- Materials in the range of $10^{-9}\ \Omega^{-1}m^{-1}$ are limited:

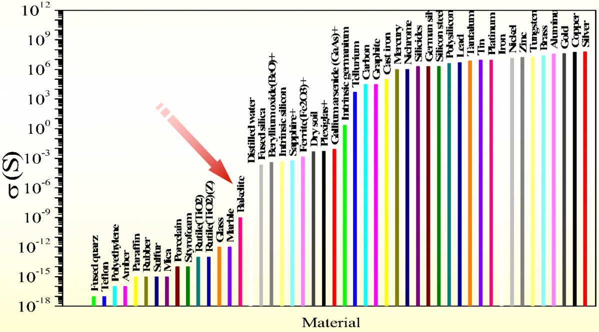

Diamond Like Carbon (DLC)

- Diamond-like carbon (DLC) is **hard, amorphous carbon film** with a significant fraction of **sp3**-hybridized carbon atoms and lower concentrations of sp2-hybrid carbon, hydrogen and dopants (N,B,...)
- The hardest DLC is tetrahedral amorphous carbon (ta-C)
- Isolator - Semiconductor - Resistive
- Wide range of applications: reduce abrasive wear & friction, engines, Hard Disks, medical app ...

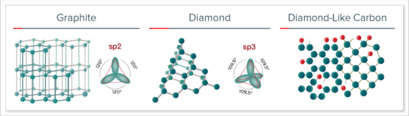

Raman Spectrum Magnetron Sputtered C-film

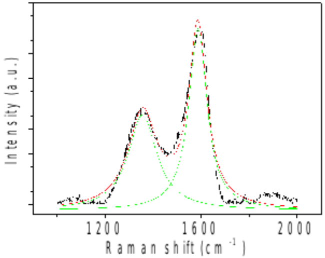

Table: Electr. param. (296 K, 100 pA)

Sheet Resistivity ($\Omega/\Box$)	$6 \cdot 10^9\ \Omega/\Box$
Bulk Resistivity (Ωcm)	590 Ωcm
Mobility (V/cm s)	564 V/cm s
Density carriers (p-type)	$1.87 \cdot 10^{13}$

Diamond Like Carbon produced in Kyoto, Japan

Traditional Resistive Material: C-black

- Carbon black loaded paste/sheet have been used for resistive material
  - Carbon black: small particles, made from mainly graphite.
  - Those are used by mixing in plastic, epoxy, solvant etc.
  - Mechanism of resistivity development

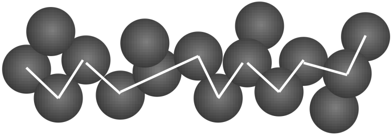

  - Carbon black particles contact each other on point, and it makes electrical path.
  - We need very small carbon black particles for fine structure of MPGD electrodes.

New Approach (in MPGD): Sputtering

- Sputtered carbon
  - Diamond like, and amorphous structure
  - It means, carbon particles of molecular size!
- Fine structure with proper resistivity is available
  - with liftoff method

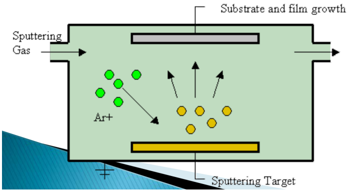

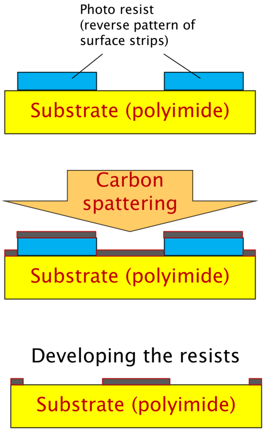

DLC Resistivity & Stability

- Resistivity dependence on carbon thickness
  - 300Å → 2GΩ/sq.
  - 3600Å → 500kΩ/sq.
  - Conductivity is not proportional to the thickness (t < 1000Å)
  - At t > 1000Å, good reproducibility found
- No time variation founds after several days from sputtering

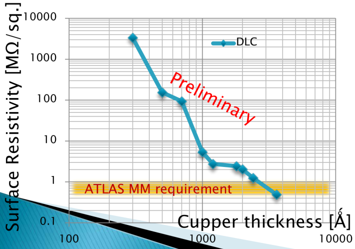

- However, deposition rate is very slow.
  - 500-600Å / hours are maximum rate in industrial chamber.
  - For ATLAS MM, 3600Å = 6hours are needed!!
  - The MSW foils were made by this longtime sputtering.
  - But **we need faster way for mass production**.

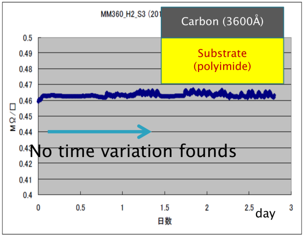

Reduce Resistivity with N-doping

- The structure of the sputtered carbon is amorphous diamond like carbon (a–DLC).
- It is thought that the charge carrier is very few in the DLC
- So, I got an idea of nitrogen doping as a supplier of carrier electrons.
  - This is same story as the n–type semiconductor production.
- The nitrogen is easy to introduce into the sputtering chamber with Argon gas.

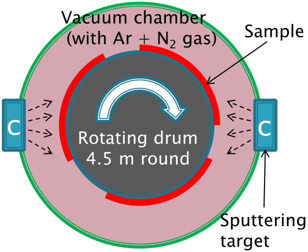

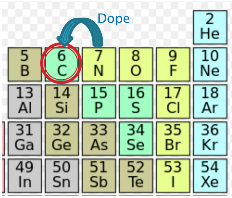

Resistivity vs Thickness

- For 3.2% N_2 content foils
  - 2400Å → 55kΩ/sq.
  - 700Å → 700kΩ/sq. (42min. sputter)

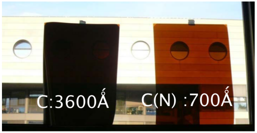

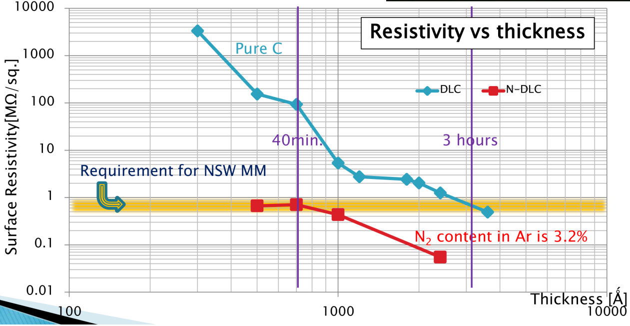

Polyimide Etching in CERN, Switzerland

Polyimide Etching Process

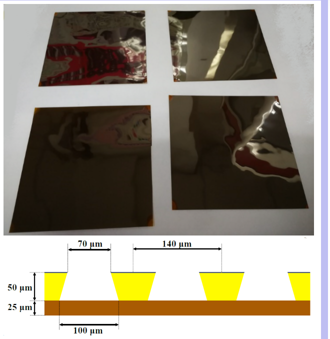

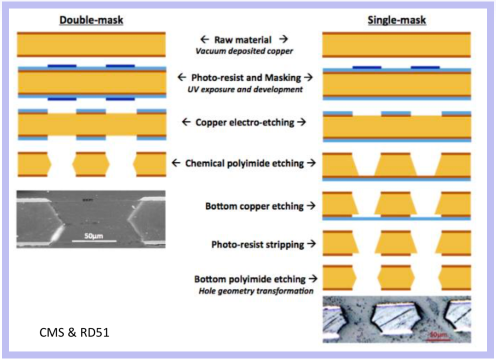

- PI-foil is one-side DLC; one-side Cu
- Single-Mask etching procedure starts on Cu clad side
- DLC side is protected from etching liquid: glued on PCB
- A well understood process (for Cu) became a very delicate process (for DLC)

FTM-v4 :: production problems

design

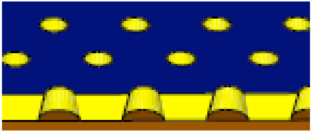

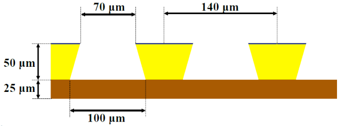

test production

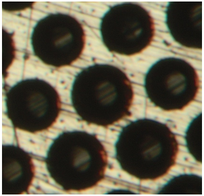

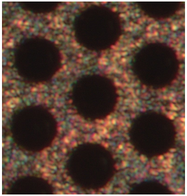

- Left: DLC top Right: Cu bottom
- DLC layer (electrode) good, but still holes way too big diameter. Holes in Cu OK.

failed production

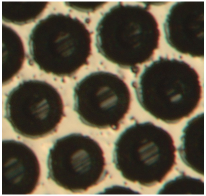

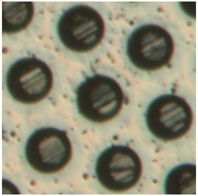

- Left: DLC top Right: PI bottom
- DLC layer (electrode) too small between two holes and breaks. Holes in PI OK.

Electric Field & Gain Simulation (I)

design DLC

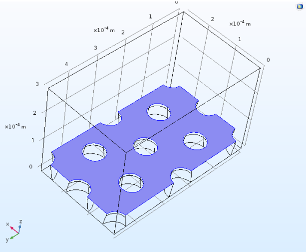

produced DLC

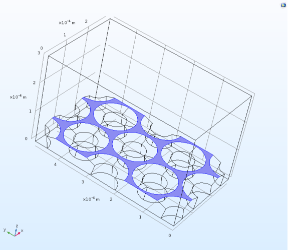

simulated E_{amp} & Gain

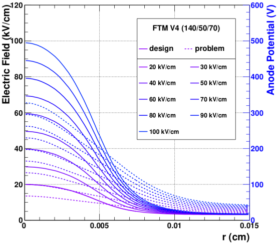

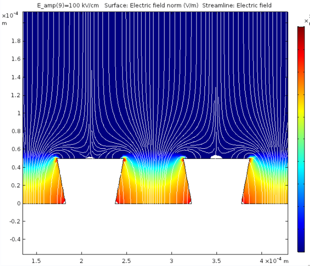

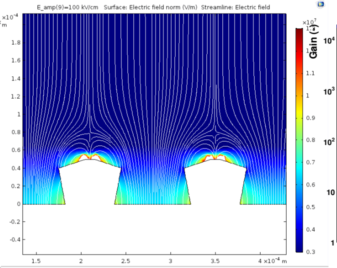

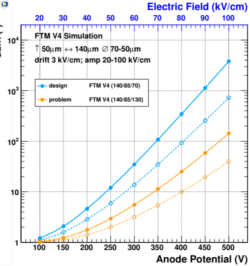

Etching problem hypothesis

- FTM amplification foil follows single-mask production process
- where Cu side of Cu/PI/DLC FCCL is used to start wet etching
- chemical Polyimide etch reaches the DLC, DLC delaminates
- chemical etch starts etching on DLC - Polyimide interface
- upon removal of DLC on holes a very small DLC electrode remains

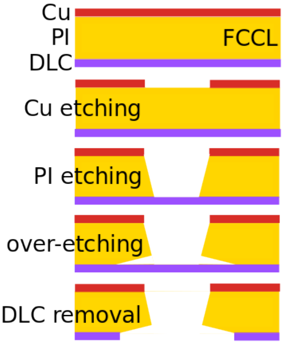

- *Rui started new production (Oct 2017), entry hole (Cu) will be reduced from 85 μm to 65 μm diameter and etching will be carefully monitored and timed to stop etching upon arrival at bottom PI and avoid over-etching. Result: bi-conical hole, not exactly what we want from point of view of high gain: instead of a gain of few 10^4 we will have only 7–8 10^3 at 550 V in Ar:CO_2 70:30.*

Electric Field & Gain Simulation (II)

produced DLC 65/45/80

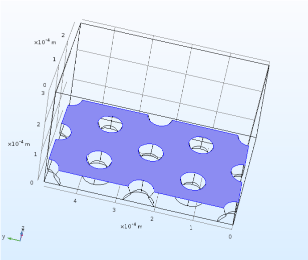

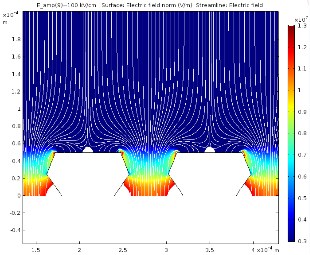

produced DLC 80/45/65

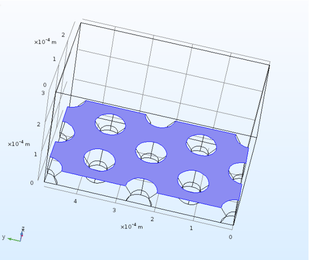

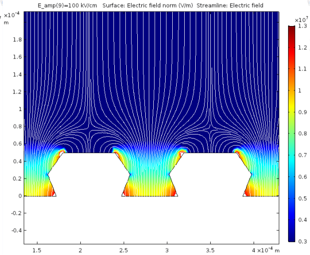

simulated E_{amp} & Gain

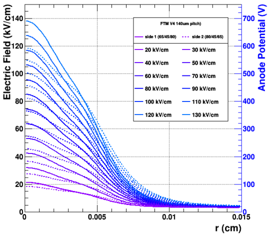

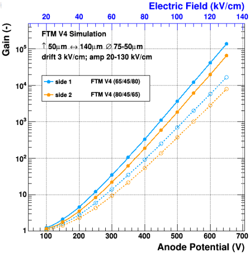

Pioneering new FCCLs

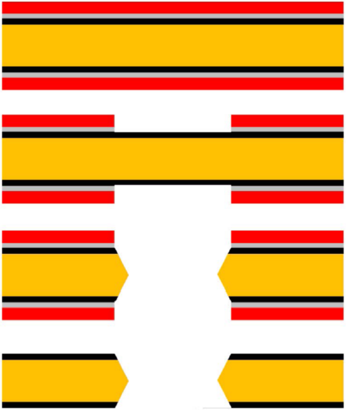

NEW FCCL: 2xDLC covered by Cu:
Cu - Cr - DLC - PI - DLC - Cr - Cu
5 - 0.1 - 0.1 - 125 - 0.1 - 0.1 - 5 (um)

Double mask etching procedure:
Cu (&Cr) photolithography + DLC sand blasting
Chemical etching of PolyImide (PI)
Removal of Cu (&Cr)

Advantages:
Can etch thicker Polyimide (up to 125um)
Allowing higher gain structures

Better protection of DLC
during etching procedure

FCCL construction procedure:
PLD of DLC, followed by PLD of Cr and Cu,
Polyimide film does not exit vacuum chamber

Idea developed during MPGD-Next by R. De Oliveira (CERN) & M. Maggi (INFN);
already adopted by USTC Colleagues (China - Magnetron Sputtering)

Diamond Like Carbon produced at USTC, China

Time Dependent N:DLC Resistivity

Long time stability in air

Measured by the multi-meter

The resistivity of the a-C:N is still increasing after 15 days, no tendency to saturate

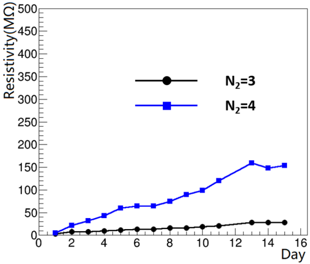

The resistivity of the a-C increased about 30% in three days, then became stable.

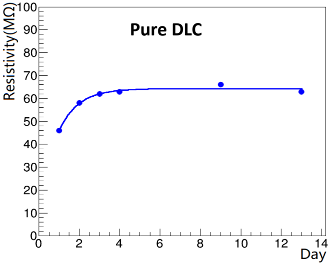

- The resistivity of the a-C/a-C:H is still stable after more than half an year

Double-sided DLC

Problems and Possible Solution

Problems in double-side coating:

- Caused extra non-uniformity of the surface resistivity;
- The maximum sample size is greatly decreased;

The edge area is closer to the target than the center area, caused the resistivity in edge area is much smaller than it in the center area

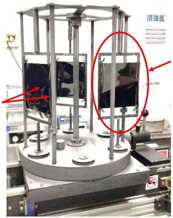

The size of the sample is limited by the space of the chamber and the structure of the rotator, the maximum size is about 15cm×15cm

Possible Solution:

- Try to add Boron into the DLC to greatly decrease the inner stress of the thick DLC foils;
- After we are able to get the thick DLC foils with low inner stress, we can use the 1-axis rotator for DLC deposition, which allow us to produce large size thick DLC samples;

Highly tetrahedral amorphous carbon films with low stress

M. Chhowalla,[a] Y. Yin,[b] G. A. J. Amaratunga, D. R. McKenzie,[b] and Th. Frauenheim[c]
Department of Electrical Engineering, University of Liverpool, Liverpool L69, 3 BX, United Kingdom

(Received 15 April 1996; accepted for publication 1 August 1996)

We have deposited boronated highly tetrahedral amorphous carbon (*ta*-C:B) films with low stress using a filtered cathodic vacuum arc. The sp^3 fraction, hardness, and resistivity were measured as a function of the ion energy and were found to reach a maximum above 50 eV for B concentrations of 2% and 4%. The most significant result we found was that highly tetrahedral *a*-C:B film (sp^3 ≈80%) with low stress (1–3 GPa) with B concentrations up to 4% could be obtained. The B in the films was found to be predominantly (≈75%) sp^2 bonded. Additionally, the stress in the films did not vary with the ion energy or sp^3 fraction unlike in regular *ta*-C films. *© 1996 American Institute of Physics.* [S0003-6951(96)01042-X]

Depositing Cu on DLC

Potentialities of Coating DLC with Copper

1. Improving the quality of current MPGDs

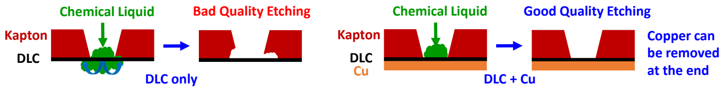

2. Allowing printed circuit layouts on DLC thus realizing complex functions

Figures come from the presentation of G. Bencivenni

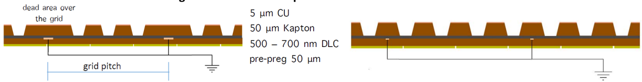

Conductive strips using screen-printing cause dead areas

DLC + Cu allow to use photolithography to greatly reduce dead areas

Coating DLC with copper can expand the capacity and applications of the MPGDs and open a way for new MPGD architectures

Depositing Cu on DLC

Depositing Copper on DLC

First Test

- Directly deposit copper on DLC for 60min

Second Test

- Coat Chrome (～100nm)on DLC
- 5min Chrome + Cu coating
- 60min Cu coating

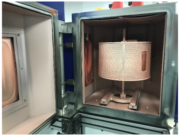

The DLC foils don't have enough toughness for attaching the Copper

The bending stress test
(Crazy kneaded by me)

The crosscut test
(Glued many times)

Adding etch-able Chrome transition layer between DLC and copper can provide good adhesion force to each interface

Diamond Like Carbon production in Lecce, Italy

FTM-Next

FTM-Next

CSN-V experiment 2019-2021

Proposal to continue R&D of the Fast Timing MPGD (FTM) based on experience and lessons learnt 2015-2018

- **Team:**
  - INFN-BA (1.3FTE) detector simulation, design & test
  - INFN-LE (1.2FTE) **DLC deposition & characterization**
  - INFN-PV (0.7FTE) detector test
- **Finances:** 130 kEUR in 3 years
- **Goals:**
  - **Reduce production time of Polyimide foils with thin DLC coating**
  - Develop procedure for DLC deposition with **reproducible resistivity** through **Pulsed Laser Deposition** process & increase DLC strength
  - **demonstrate FTM principle with small-size prototype**
  - Continue **Fast Electronics** development for smal signals (1.6 fC)

High Quality Thin DLC films through PLD

- **Deposition of Uniform Low-Resistivity DLC layers:** **(Core)**
  - in a reproducible way;
  - with good thickness uniformity (hence good resistivity uniformity);
  - with good adhesion of DLC to polyimide;
  - with application-taylored surface resistivity values (Rate vs Res.).
- **Pulsed Laser Deposition:**
  - good control of DLC properties thanks to independent PLD param.;
  - will allow for fast iteration to converge to reproducible results
- **Characterization of DLC films:**
  - AFM & SEM to study morphology & topography of DLC;
  - DLC-PI bond & DLC internal stress investigated through Raman spectroscopy; 4-point Hall probe to characterise electrical properties
- **Excellent expertise in field of Thin Films in Italy (Lecce)**

Detector Construction & Tests

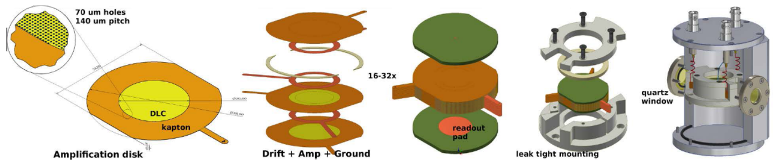

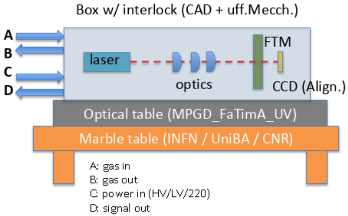

CryLaS GmbH — *Crystal Laser Systems* — Committed to light.

FQSS 266-50

Diode pumped passively Q-switched solid state laser

- **266 nm**
- **single pulse**
- **0.9 - 1.3 ns**
- **1 – 100 Hz** (up to 1 kHz optional)
- **> 50 μJ**

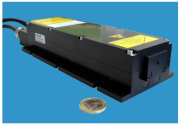

biology · biomedicine · chemistry · analytics

Optical Data		
	Wavelength	266 nm
	Spatial Mode	TEM_{00}
	M^2	< 1.5
	Beam Divergence (full angle)	< 3.0 mrad
	Beam Ellipticity	< 1.5:1
	Waist Diameter	800 ± 200 μm (located at about 110mm inside the laser head)
	Beam Diameter	800 ± 200 μm (at laser exit)

Gaseous Detectors for Future Colliders

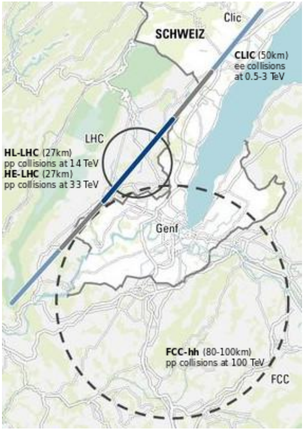

- Future Colliders (FC) will operate at higher $\sqrt{s}$ and $\mathcal{L}$
- For muon detection systems of FC experiments:

  $\frac{\Delta p}{p} \propto \frac{1}{BL^2} \Rightarrow$ high B field, large instrumented area

  $\mathcal{L} \Rightarrow$ higher rate capability, Pile-Up vertices
- To **instrument large areas**, gas detector technology will remain unchallenged
- Detectors need to have **high rate capability**
- **Fast Timing will enable to identify the correct interaction** (as many as 1000 collisions will overlap with the interesting collision = Pile-Up)

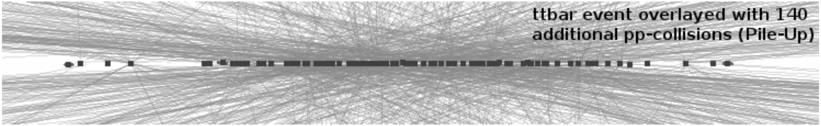

Time-Of-Flight Positron Emission Tomography

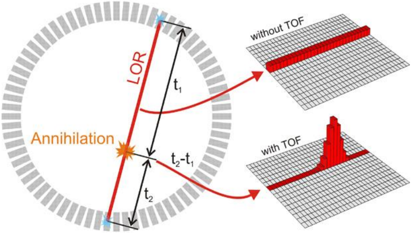

PET principle, w/ & w/o TOF. [source: `sublima-pet-mr.eu/`]

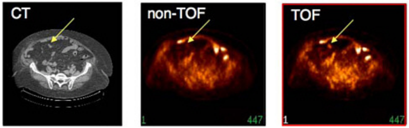

PET scans of a patient with colon cancer. The use of TOF improves the lesion detectability (arrow). [source: J. Karp, U. Pennsylvania.]

PET is a technique to visualize organs with **high metabolic activity** and is used to spot tumors

- β^+ sugar (FDG) is administered to a patient and concentrates at regions of high metabolic activity (tracer)
- e^+ is released and looses energy during travel ($\sim$1 mm) before annihilation
- $2\ \gamma$ (511 keV) are emitted back to back, their coincident detection determines the Line of Response (LOR)
- w/o TOF equal probability assigned to each point along the LOR
- w/ TOF few 100 ps measurement will lead to $\sim$ 5 cm precision along the LOR

the use of fast timing in PET results in high contrast images

Acknowledgments

I would like to thank ...

- **Atsuhiko Ochi, Yi Zhou & Gianni Bencivenni** for the material (slides) I flagrantly stole;
- **Silvia Franchino** whose contributions in the early days of the project were fundamental for the study and construction of the first prototypes;
- **Ilaria Vai, Francesco Fallavolita, Martina Ressegotti, Lisa Borgonovi & Federica Simone** who dedicated lots of hours in testing the early FTMs in the lab and with beam;
- **Giuseppe De Robertis & Francesco Licciulli** for desiging and testing the FATIC electronics;

- **Antonio Ranieri & Anna Paola Caricato** for their trust and endless stimulation;
- **Archana Sharma**, **Marcello Maggi** and **Rui De Oliveira**, mother and fathers of the FTM for their continuous support.

Questions?

Backup:

- Amplification Structures
- DLC for ATLAS NSW MM
- FTM-v1 Results
- TOF-PET FTM Simulations

Amplification Structure: Resistive μ-WELLs

FTM

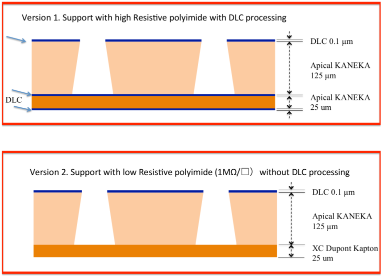

μ-RWELL

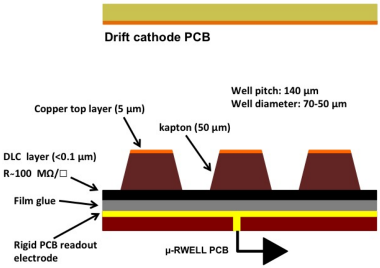

- By constr: FTM *inverted* hole (50-70 μm), μ-RWELL *normal* hole (70-50 μm)
- **Electric Field** calculation in gas **very similar** (independent of base details)
- FTM (multip. layers) $\Rightarrow$ micro-gap (250 μm); while 3–4 mm drift for μ-RWELL

ATLAS New Small Wheel Upgrade

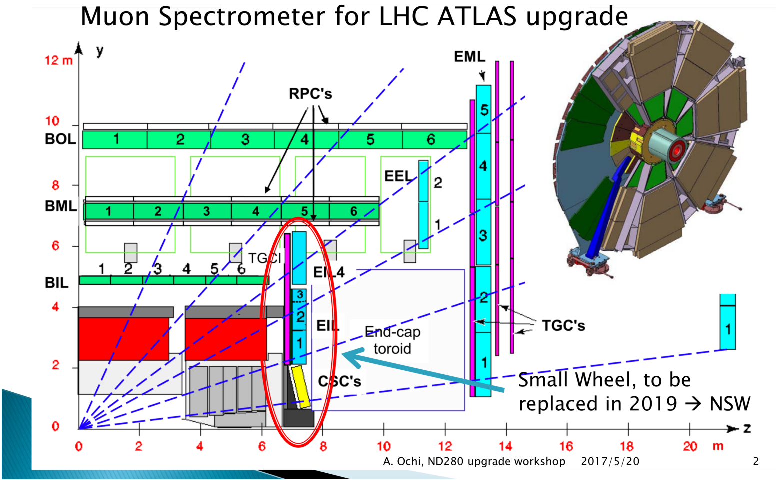

DLC Sputtering vs Carbon Screen Printing

Two options for resistive electrodes of ATLAS MM

- Sputtering+liftoff
  - Pros.
    - Large area (>2m)
    - Fine pattern (<100µm)
    - Uniform resistivity
    - Strong attachment on substrate
  - Cons.
    - Production speed (Now, it will be OK, next slide)
    - High cost
- Screen printing
  - Pros.
    - Large area (>2m)
    - Fast production speed
    - Low cost for mass production
  - Cons.
    - Stability of resistivity
    - Thick pattern (~20 µm)
    - Lower tolerance for breakdown for high voltage

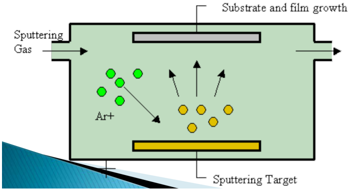

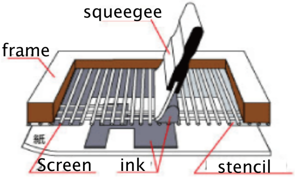

Trials of Different Resistive Materials 1

Our experiences of resistive materials

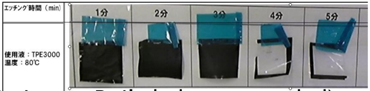

- Resistive Polyimide sheet
  - Dupont Kapton XC series
  - Commercially available (not in Japan, Rui's help was needed)
  - Typically, 2MΩ/sq. , 25μm thickness
- Resistive polyimide paste
  - Produced in Toray
  - It is not commercially available
  - A few MΩ/sq. , 10–20μm thickness
- Resistive epoxy paste
  - ESL RS12500 series
  - Commercially available
  - Typically, 1MΩ/sq. , 10μm thickness
- Carbon sputtering
  - Carbon deposition by dry sputtering
  - 100kΩ/sq. – 100MΩ/sq. , 0.1μm thickness

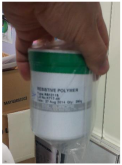

Trials of Different Resistive Materials 2

Summary

- Various resistive materials were tested for μ-PIC, MM and GEM prototypes.
- For fine structure, photo lithographic method is suitable.
  - Most fine structure will be formed by carbon sputtering
  - Also huge size (>1m) production is available
- Screen print of resistive paste is very low cost
  - Less fine, but it is enough to ATLAS NSW MM resistive strip

Materials	Resistive sheet	Paste (polyimide)	Paste (epoxy)	Sputter
Resistivity	2M	1M~2M	0.5M~2M	50k~100M
Fineness	~50μm	~100μm	~100μm	~10μm
Process	Etching Laser drilling	Liftoff Screen print	Screen print	Liftoff Laser drilling
Detector	μ-PIC GEM (RIKEN)	μ-PIC MicroMEGAS	MicroMEGAS	μ-PIC MicroMEGAS GEM

First FTM Prototype (FTM-v1) :: Results

Simulations & SPS Test-beam Results [M. Maggi & I. Vai]

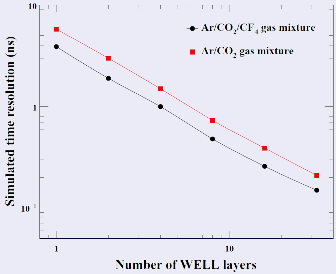

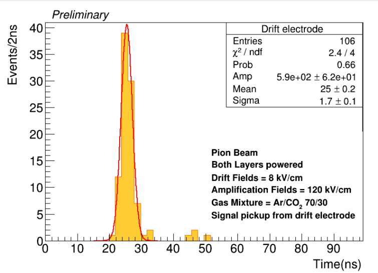

[source: arXiv:1503.05330] [source: NIM A 845 (2017) 313]

- Simulations show time resolution decreasing for increasing number of layers
- Pion Test Beam for 2 layer prototype shows time resolution of 1.7±0.1 ns
- Muon Test Beam for 2 layer prototype shows time resolution of 2.4±0.1 ns
- $\sigma_t = 1/(\lambda v_{\text{drift}} N)$ with $\lambda^{\text{MIP}}_{\text{Ar/CO}_2\ 70/30} = 25\,\text{cm}^{-1}$, $v_{\text{drift}} = 8\,\text{cm}/\mu\text{s}$, $N = 2 \Rightarrow \sigma_t = 2.5\,\text{ns}$

TOF-PET FTM Simulations

Fast Timing MPDG for photons

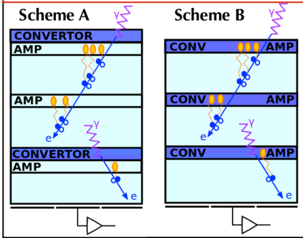

- Adapt structure to detect 511 keV γ from PET
- Two scheme under study:
  - A. photon converted in high-Z resistive material + several thin amplification layers
  - B. γ can convert in each amp. layer (only resistive material allowed)
- Sub-relativistic e^- has high ionization density
- inverted order of drift and gain region → fast signal

- Simulation split in two steps:
  1. Search for optimal resistive convertor material and extract electron energy distribution at exit material
  2. Simulate Primary Ionization of sub-relativistic electron and extract expected time-resolution
- Simulate two-amplification layer (Scheme A) to understand whether electron can perforate thin amplification structure to decide between scheme-A and scheme-B

Photon Conversion

- Study to guide design of FTM for PET scheme, materials, geometry, …
- GEANT4.10.03 version used
- FTFP_BERT_HP physics list
- Simulation of 511 keV γ interaction in different materials and thicknesses:
  - PCB (FR4), kapton, glass (G4_GLASS_LEAD), lead glass (G4_GLASS_PLATE)

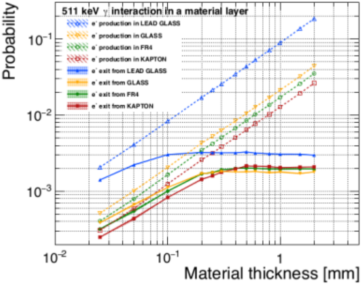

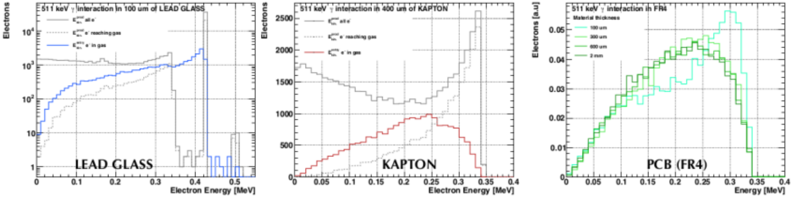

511 keV γ conversion in different materials is studied. Electron production probability and energy spectra for electrons entering the drift region.

Sub-relativistic Electron Ionization

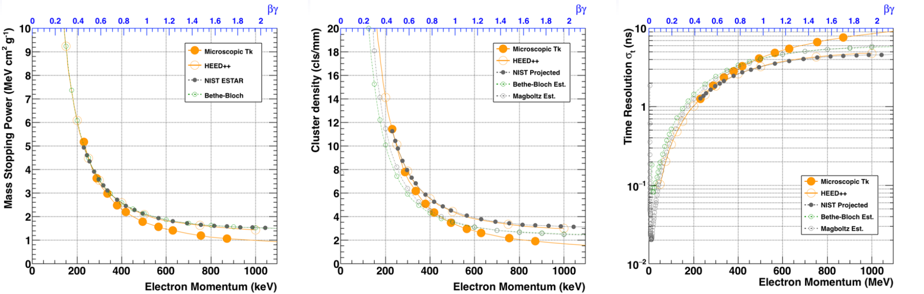

- Search for right approach to simulate the ionization of sub-relativistic electrons
- **HEED gives good agreement with NIST ESTAR and Bethe-Bloch**
- Garfield Microscopic Tracking (Magboltz cross sections) ok for low-energy
- Time resolution estimate made for single-layer FTM with convertor:
- Electron Momentum: 50 keV - 200 keV – 300 keV :: 100 ps – 1 ns – 2 ns